MAXIMUM LIKELIHOOD METHODS FOR BEARINGS-ONLY TARGET LOCALIZATION

Lance M. Kaplan[1,3] *Qiang Le*[2,3] *Péter Molnár*[2,3]

[1]Dept. of Engineering [2]Dept. of Computer Science
[3]Center for Theoretical Studies of Physical Systems
Clark Atlanta University
Atlanta, GA 30314

ABSTRACT

In this work, we develop four maximum likelihood (ML) methods to localize a moving target using a network of acoustical sensor arrays. Each array transmits a direction-of-arrival (DOA) estimate to a central processor, which employs one of the localization techniques. The four ML approaches use different target signal models where the time retardation factor for the target position and the degradation of the target signal through the air may or may not be included in the model. We compare these methods along with a linear least squares approach through a number of simulations at various signal to noise levels.

1. INTRODUCTION

Bearings-only target localization techniques provide a key ingredient to the development of an unattended ground sensor (UGS) network. The military is interested in UGS technology because it promises to provide a low cost, low power and high performance solution for battlefield surveillance. The network is attractive because it can act as one giant array. However, bandwidth is limited because the transmission of a bit of information between nodes drains much more battery power than a single computation on each node's processor. In order to conserve energy, some nodes generate and transmit a direction-of-arrival (DOA) estimate to a node that is acting as the central processor. The central node processes the bearing information to localize and track targets of interest. A distributed sensor management strategy dynamically designates the active nodes and assigns nodes the central processing task.

In this paper, we describe and test four maximum likelihood (ML) techniques that localize (or triangulate) a moving target traveling through a passive acoustical UGS network. Each node is a very small baseline array of omni-directional microphones configured in a wagon wheel pattern as shown in Figure 1a. Previous methods to triangulate a stationary target via active electromagnetic sensors are presented in [1]. One such method is one of the four ML localization techniques considered in this paper. However, this particular estimator assumes that the target is stationary. Because the speed of sound is not orders of magnitude greater that the target's speed, we develop two alternative ML localization techniques that account for the target's velocity. Similar to the large baseline acoustical tracker presented in [2], these techniques uses a time retardation factor to account for the movement of the target during the propagation of the signal [2]. All four localization techniques provide estimates that can be used as measurements for a tracker such as the Kalman filter.

Prepared through collaborative participation in the Advanced Sensors Consortium sponsored by the U.S. Army Research Laboratory under Cooperative Agreement DAAL01-96-2-0001. The U.S. Government is authorized to reproduce and distribute reprints for Government purposes notwithstanding any copyright notation thereon.

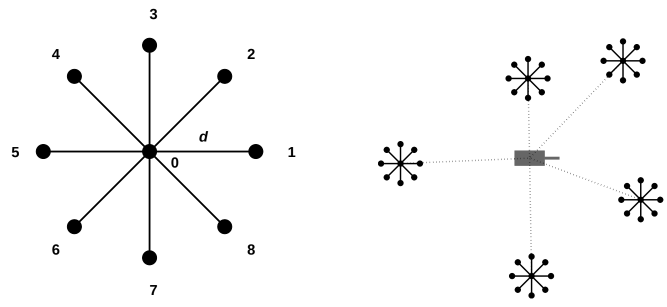

Fig. 1. The geometry of the acoustical UGS: (a) The single node, and (b) triangulation using multiple nodes.

This paper in organized as follows. Section 2 describes the geometry of the single UGS node as well as the network and discusses the DOA errors. These errors leads to the target model that is presented in Section 3. Section 4 introduces the linear least squares (LLS) localization technique. Then, Section 5 develops the ML localization technique for the target model of Section 3 and other ML techniques for various simplifications of this model. This section also discusses the Cramer-Rao bounds for these ML methods. The paper compares the different localization algorithms through Monte-Carlo simulations as described in Section 6. Finally, Section 7 provides some concluding remarks.

2. UGS GEOMETRY

For this paper we consider a UGS network of only acoustical sensors. As shown in Figure 1a, each UGS node is an acoustical array consisting of $M = 9$ omni-directional microphones where $M - 1$ sensors are distributed evenly over a circle of radius $d = .1$ meters around the central sensor. The central microphone is labeled as sensor $i = 0$, and the other $M - 1$ outer sensors are labeled $i = 1, 2, \dots, M-1$. Each sensor of the UGS samples an acoustic signals $f_i(t)$. A DOA algorithm exploits time of arrival differences from N samples of signal $f_i(t)$ to extract the bearing estimate. An expression for the variance of DOA estimates using the MUSIC algorithm for a narrowband target signature appears in Eqn. (42) of

[3]. Simplification of this expression for the geometry in Figure 1a leads to an error variance of

$$\sigma_\theta^2 = \left(\frac{\lambda}{2\pi d}\right)^2 \frac{M \cdot \mathrm{SNR} + 1}{M(M-1)N \cdot \mathrm{SNR}^2}, \tag{1}$$

where λ is the wavelength of the narrowband target signature and SNR is the signal to noise ratio.

The geometry of the UGS network is illustrated in Figure 1b. The locations of the N_s sensor nodes are labeled $\vec{S}_i = (S_{x,i}, S_{y,i})^T$ for $i = 1, \ldots, N_s$. Note that the sensor nodes are stationary. The target is moving through the sensor field. The position and velocity of the target at time t is $\vec{P}_t = (P_{x,t}, P_{y,t})$ and $\vec{V}_t = (V_{x,t}, V_{y,t})^T$, respectively. At well defined time increments, which we refer to as *snapshots*, all the functional nodes collect their DOA estimate and send it to a designated central processing node. The central node applies a localization algorithm to estimate the position, and possibly the velocity, of the target.

3. THE TARGET MODEL

The target model represents the DOA estimate at each node for one snapshot as the true bearing angle embedded in additive Gaussian noise, i.e.,

$$\hat{\theta}_i = \theta_i + n_i, \tag{2}$$

where $n_i \sim N(0, \sigma_i^2)$. For simplicity, we set the snapshot time to be $t = 0$. We assume that the nodes are sufficiently separated so that the noise terms n_i are independent. The true bearing angle reflects the location of the target at the retarded time when it emitted the signal that is processed by the sensor node The localization algorithms assume that the velocity of the target is constant over the largest retardation time so that $\vec{P}_t = \vec{P}_0 + t\vec{V}$. For the constant velocity target, the retarded time is given by

$$\tau_i = -\frac{\left(\vec{D}_i^T\vec{V} + \sqrt{\left|\vec{D}_i^T\vec{V}\right|^2 + (c^2 - v^2)\vec{D}_i^T\vec{D}_i}\right)}{c^2 - v^2},$$

where $\vec{D}_i = \vec{S}_i - \vec{P}_0$, $c = 347$m/s is the speed of sound and $v = \|\vec{V}\|$ is the speed of the target. Because v is a significant fraction of c, the target can move appreciably from the retarded to snapshot time. The true bearing angle becomes

$$\theta_i = \angle(\vec{P}_{\tau_i} - \vec{S}_i).$$

The variance of the additive noise σ_i^2 is an increasing function of the distance between the sensor and the retarded target location. This is due to the relationship between the bearing error and SNR in (1), and the SNR degrades as the target signal propagates through the air. The degradation of SNR along a particular path is a complex function of the meteorological conditions. At this time, we assume that the degradation of the SNR follows a $1/r^2$ law. As a result, the error variance is

$$\sigma_i^2 = \left(\frac{\lambda}{2\pi d}\right)^2 \frac{1}{N(M-1)} \left(\frac{r_i^2}{\mathrm{SNR}_0} + \frac{r_i^4}{M \cdot \mathrm{SNR}_0^2}\right), \tag{3}$$

where $r_i = \|\vec{S}_i - \vec{P}_{\tau_i}\|$ and SNR_0 is the normalized SNR at a distance of one meter.

4. LINEAR LEAST SQUARES LOCALIZATION

The **position linear least squares** (P-LLS) localization method assumes that the target is stationary and that the bearing estimate points in the direction of the target. For sensor i, the target must be located on the line described by

$$\tan\hat{\theta}_i x + y = S_{i,x}\tan\hat{\theta}_i + S_{i,y}.$$

Using all sensors leads to N_s linear equations and two unknowns. Because of the DOA estimation error, an exact solution for the N_s equations does not exist in general. To compensate for these errors, we use the least squares solution of the N_s equations as the localization estimate so that

$$\hat{P}_0 = (A^T A)^{-1} A^T \vec{b},$$

where

$$A = \begin{pmatrix} \tan\hat{\theta}_1 & 1 \\ \vdots & \vdots \\ \tan\hat{\theta}_{N_s} & 1 \end{pmatrix} \quad \text{and} \quad \vec{b} = \begin{pmatrix} S_{1,x}\tan\hat{\theta}_1 + S_{1,y} \\ \vdots \\ S_{N_s,x}\tan\hat{\theta}_{N_s} + S_{N_s,y} \end{pmatrix}.$$

5. MAXIMUM LIKELIHOOD ESTIMATION

In this section, we develop four ML localization algorithms based upon various simplifications of the target model from Section 3. These ML techniques are:

- **Position-Velocity ML (PV-ML):** The ML estimator for the target model in Section 3. This technique assumes the target is moving at a constant velocity and the DOA measurement error degrades via (3) as the distance to the target increases. The position and velocity estimates, $\hat{\vec{P}}_0$ and $\hat{\vec{V}}$, minimize the following cost function

$$C_{PV-ML} = \sum_{i=1}^{N_s} \left(\frac{1}{\sigma_i^2}|\hat{\theta}_i - \angle(\vec{S}_i - \vec{P}_{\tau_i})|^2 + \ln\sigma_i^2\right).$$

- **Position ML (P-ML):** The ML estimator when the target is assumed to be stationary and the DOA measurement error degrades via (3) as the distance to the target increases. For this model, the time retardation factor is ignored. The position estimate $\hat{\vec{P}}$ minimizes the following cost function

$$C_{P-ML} = \sum_{i=1}^{N_s} \left(\frac{1}{\sigma_i^2}|\hat{\theta}_i - \angle(\vec{S}_i - \vec{P})|^2 + \ln\sigma_i^2\right).$$

- **Position-Velocity Nonlinear Least Squares (PV-NLS):** The ML estimator when the target is moving at a constant velocity and the measurement error is the same for every sensor in the network. The position and velocity estimates, $\hat{\vec{P}}_0$ and $\hat{\vec{V}}$, minimize the following cost function

$$C_{PV-NLS} = \sum_{i=1}^{N_s} |\hat{\theta}_i - \angle(\vec{S}_i - \vec{P}_{\tau_i})|^2.$$

- **Position Nonlinear Least Squares (P-NLS):** The ML estimator when the target is stationary and the measurement error is the same for every sensor in the network. For this model, both the time retardation factors and the sensor/target distances are ignored. The position estimate $\hat{\vec{P}}$ minimizes the following cost function

$$C_{P-NLS} = \sum_{i=1}^{N_s} |\hat{\theta}_i - \angle(\vec{S}_i - \vec{P})|^2.$$

This algorithm has already been developed for bearing-only localization using electro-magnetic signals [1, 4]. When applied for electro-magnetic signals, the speed of light is significantly larger than the target velocity. Therefore, the triangulation methods presented in the electro-magnetic literature ignore the time retardation effects because they are insignificant.

All four ML techniques require an initial guess for the location of the target. In addition, the PV methods also require an initial guess for the target velocity. To find the minima from the initial guess, we employ the Nelder-Mead simplex (direct search) method, which is implemented via the `FMINS` command in `Matlab`. As an initial comparison of the different methods, we use the actual parameter values to search for the nearest local minima, which should correspond to the global minima. In practice, the localization algorithms require an intelligent approach to initialize the search. As the target model becomes more sophisticated, the resulting ML decision surface becomes more complex and more sensitive to the initialization. Therefore, to initialize the PV-ML, we begin with the P-LLS position estimate and minimize the P-NLS cost function. The resulting position estimate and a zero velocity initializes the PV-NLS search. Finally, the PV-ML estimates are obtained by initializing with the output of the PV-NLS.

We have determined expressions for the Cramer Rao (CR) bounds for the four ML localization techniques. The bound for the PV-ML method is

$$C(\vec{P}_0, \vec{V}) = \left[\sum_{i=1}^{N_s}\left(\frac{(\nabla_P \sigma_i^2)(\nabla_P \sigma_i^2)^T}{2\sigma_i^4} + \frac{(\nabla_P \theta_i)(\nabla_P \theta_i)^T}{\sigma_i^2}\right)\right]^{-1}, \tag{4}$$

where the true angle $\theta_i = \angle(\vec{S}_i - \vec{P}_{\tau_i})$ and $\nabla_P = [\frac{\partial}{\partial P_{x,0}}, \frac{\partial}{\partial P_{y,0}}, \frac{\partial}{\partial V_x}, \frac{\partial}{\partial V_y}]^T$.

Due to space considerations, we do not include expressions for the gradients of the DOA error variance and the true angle, and we do no include the CR bounds for the other three ML techniques. The diagonal of the covariance matrix C represents the lower bound for the estimation error variance of the target position and velocity parameters. These bounds are a function of the sensor configuration $\vec{S}_i$ and the target's position and velocity at the time of the snapshot.

6. SIMULATION RESULTS

To demonstrate the localization approaches, we ran a number of simulations using the target model described in Section 3 where the target emits a 100Hz narrowband signature so that $\lambda = 3.5m$ and each microphone collects $N = 100$ samples of the received signal to obtain the DOA estimate. The number of nodes N_s varies from four to forty. For a set value of N_s, we consider 20 different random configurations where the sensors are uniformly distributed in a circle of radius 0.5 km around the target and the target is traveling at a speed of 48 km/hr (30 mi/hr) in a random heading. We normalize the SNR at a one meter standoff range to either 90dB or 60dB, which leads to an average bearing error of about $0.1°$ or $3.5°$, respectively. For each configuration, we run 50 Monte Carlo simulations to obtain the root mean squared (RMS) error for the position and speed estimates. In addition, we use the CR bound

N_s	Initialization	Avg.	Min.	Median	Max.
5	P-LLS	7.7096	0.6225	5.8119	18.5457
5	True Value	6.2213	0.0002	2.0833	18.5456
14	P-LLS	22,230	278.00	450.55	111,599
14	True Value	0.6177	0.0001	0.2133	1.8558

Table 1. Statistics for the RMS position error of the sensor filed configuration in Figure 3.

from (4) to estimate the RMS lower bounds for position and speed as

$$\text{RMS}\{p\} \approx \sqrt{C_{1,1} + C_{2,2}} \quad \text{and} \quad \text{RMS}\{v\} \approx \sqrt{C_{3,3} + C_{4,4}}, \tag{5}$$

respectively. We then average these results over the 20 different configurations to generate performance plots as function of number of nodes.

When the true target parameters are used at the initial condition for the search, the four ML methods should converge to the global minimum. The results using true value initialization are presented in [5]. They indicate that at high SNR the time retardation factor makes a significant difference at a high SNR (90dB) while the signal degradation factor is less important. As mentioned in Section 5, we are currently using a cascade of the P-LLS, P-NLS and PV-NLS localizations to initialize PV-ML technique. Figures 2a and b show the position RMS error results after each stage for 90dB and 60dB normalized SNR, respectively. Due to space limitations, we do include the velocity RMS error results. These figures also include the bounds. When $N_s \leq 10$, the PV-ML converges to the best estimate. However, for some larger values of N_s, the likelihood techniques converged to poor results where the result is worst as the sophistication of the model increases. The bad estimates were the result of a few outlier configurations. An example of such a configuration when $N_s = 14$ is shown in Figure 3. The '$\times$' markers represent the sensor nodes, the '$\diamond$' represents the target, and the line originating form the target indicates the target heading. Figures 2c and d show the results when removing the problem configurations from the averaging. Most of the time, the PV-ML method provides the best localization at 90dB. At low SNR, the likelihood methods never perform significantly better than the P-LLS technique.

The poor PV-ML results when $N_s > 10$ could be attributed to a more complex cost function so that the searching method does not find the global minimum. In fact, a subset of the nodes can allow the PV-ML to converge to a better answer in practice. As an example, we use only a subset of nodes in Figure 3 as labeled by the '$\circ$' symbols. The statistics for the RMS position error is listed in Table 1 when using all nodes or the five node subset for both the realizable initialization beginning with the P-LLS or using the true target position and velocity parameters for initialization. While the full set of nodes leads to a minima closer to the true value, the practical PV-ML finds a better minima for the five node subset.

7. CONCLUSIONS

This paper investigates a number of ML techniques to triangulate the position of a target using bearings-only measurements from an acoustical UGS network. For high SNR cases, the localization technique should consider time retardation factors. For low SNR cases, however, the time retardation factor is less important. Unfortunately, the estimates are sensitive to good initialization of the

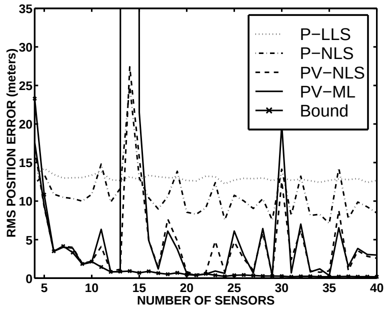

(a)

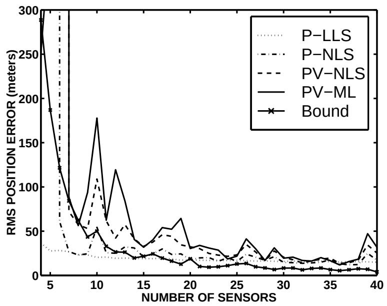

(b)

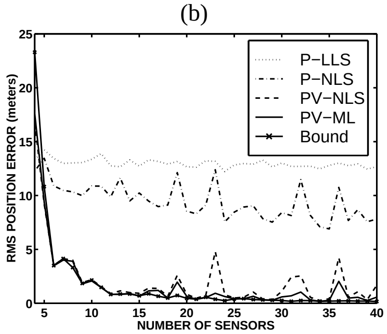

(c)

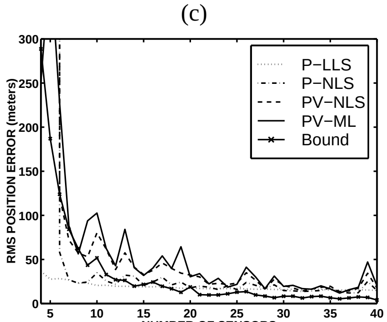

(d)

Fig. 2. Simulation results that begin initialization with the P-LLS algorithm: (a) Position RMS for $\text{SNR}_0 = 90$dB, (b) position RMS for $\text{SNR}_0 = 60$dB, (c) position RMS for $\text{SNR}_0 = 90$dB with outlier removal and (d) position RMS for $\text{SNR}_0 = 60$dB with outlier removal.

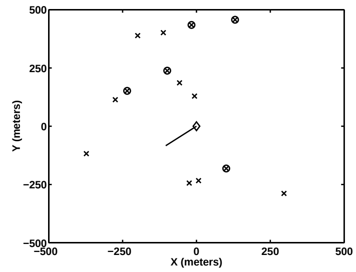

Fig. 3. Example of the bad sensor configuration when $N_s = 14$. The realizable PV-ML performs better over a subset of five nodes.

minimization method. In the future, we plan to research better ways to initialize the ML algorithms and include other modification in order to localize multiple targets. One such method is to develop a tracker where the output of the localization algorithm at multiple snapshots provides the tracking input measurements. As the time progresses, the tracker should predict better estimates of the target parameters, which in turns, leads to a lower occurrence of converging to poor localization estimate. To save power, we also plan to work on sensor management methods that find the best subset of nodes to activate during each snapshot. Limiting the number of active nodes to less than ten should also alleviate the initialization problem.

8. REFERENCES

[1] Yaakov Oshman and Pavel Davidson, "Optimization of observer trajectories for bearings-only target localization," *IEEE Trans. on Aerospace and Electronic Systems*, vol. 35, no. 3, pp. 892–902, July 1999.

[2] Kam W. Lo and Brian G. Ferguson, "Broadband passive acoustic technique for target motion parameter estimation," *IEEE Trans. on Aerospace and Electronic Systems*, vol. 36, no. 1, pp. 163–175, Jan. 2000.

[3] A. Lee Swindlehurst and Thomas Kailath, "A performance analysis of subspace-based methods in the presence of model errors, Part I: The MUSIC algorithm," *IEEE Trans. on Signal Processing*, vol. 40, no. 7, pp. 1758–1773, July 1992.

[4] S.C. Nardone, A. G. Lindgren, and K. F. Gong, "Fundamental properties and performance of conventional bearings-only target motion analysis," *IEEE Trans. on Automatic Control*, vol. 29, pp. 775–787, Sept. 1984.

[5] Lance M. Kaplan, Qiang Liang, and Péter Molnár, "Fusion of bearing measurements from acoustical unattended ground sensors for target localization," To appear in *Proc. of the 2001 ARL Federated Laboratory Symposium*, Oct. 2001.

[1]The views and conclusions contained in this document are those of the authors and should not be interpreted as presenting the official policies either expressed or implied of the Army Research Laboratory or the U.S. Government.